

Localization transition in symmetric random matrices

F. L. Metz, I. Neri and D. Bollé

Instituut voor Theoretische Fysica, Katholieke Universiteit Leuven, Celestijnenlaan 200D, B-3001 Leuven, Belgium

(Dated: October 24, 2018)

We study the behaviour of the inverse participation ratio and the localization transition in infinitely large random matrices through the cavity method. Results are shown for two ensembles of random matrices: Laplacian matrices on sparse random graphs and fully-connected Lévy matrices. We derive a critical line separating localized from extended states in the case of Lévy matrices. Comparison between theoretical results and diagonalization of finite random matrices is shown.

PACS numbers:

I. INTRODUCTION

Since the pioneering work of Wigner in nuclear physics [1], random matrices have been intensively studied due to their wide range of applications in several fields of physics and other disciplines. Some examples include quantum chaos [2], localization in electronic systems [3], diffusion in random graphs [4, 5], finance [6, 7] and complex networks [8].

In random matrix theory, one is interested in physical quantities that can be computed from the eigensolutions of a sample drawn from an ensemble of $N \times N$ random matrices. One of the main quantities of interest is the density of states (DOS). In the case of the Gaussian orthogonal ensemble the DOS obeys the Wigner semicircle law in the limit $N \rightarrow \infty$ [9]. There are several ensembles in which the average DOS differs from the semicircle law in a nontrivial way. The examples include the ensemble of sparse matrices [10–15], Laplacian matrices [5, 16–19] and Lévy matrices [20–22]. Finite size effects do not play a significant role and the DOS converges to its large N limit relatively fast.

Another important quantity is the inverse participation ratio (IPR) since it provides valuable information about the nature of the eigenstates. The IPR allows one to quantify the number of nonzero components in a certain eigenvector in the limit $N \rightarrow \infty$. It is a suitable parameter to describe quantitatively a delocalization-localization transition, since it distinguishes between eigenstates that have a finite number of nonzero components (localized states) and eigenvectors that have an extensive number of nonzero components (extended states). The critical eigenvalue separating localized from extended states is called the mobility edge or the localization threshold. The mobility edge determines the Anderson transition in electronic systems [3] and the emergence of particle traps in diffusion models on random lattices [4, 5]. An equation that determines the mobility edge in the ensemble of sparse random matrices was obtained by means of the supersymmetric method [23]. Within our knowledge there exists no full numerical solution for the mobility edge by calculating the IPR with the supersymmetric method.

In contrast to the DOS, numerical diagonalization results show a significant dependence of the average IPR

upon N [14, 16, 17]. Moreover, since localized states are usually present in the tails of the spectrum of random matrices, one would have to diagonalize extremely large matrices to detect these states. In order to determine the localization threshold in the limit $N \rightarrow \infty$, the imaginary part of the self-energy [3] and the variance of the density of states [24, 25] have been proposed as appropriate parameters. However, a more quantitative description of the localization transition would be obtained by calculating the average IPR for infinitely large random matrices.

Laplacian matrices on sparse random graphs [16] and fully-connected Lévy matrices [20] are two examples of random matrices in which results for the average IPR as a function of the eigenvalue have been obtained only through diagonalization of finite matrices. Laplacian random matrices arise, e. g., in the study of diffusion on random graphs [4, 5, 18] and in the instantaneous normal modes approach for liquid dynamics [17]. Lévy random matrices appear, e. g., in models of spin-glasses with dipolar RKKY interactions [26], in the study of disordered electronic systems with interactions decaying as a power-law of the distance [20], in portfolio optimization [27] and in the study of correlations in data, for instance, coming from financial time series [28, 29].

In this work we calculate the eigenvalue-dependent IPR from the Green function corresponding to the random matrix in the limit $N \rightarrow \infty$. The cavity method provides a self-consistent equation for the Green function, which is easily solved through a population dynamics algorithm [30]. This approach is free of finite-size effects and it can be used to study the average IPR of different ensembles of infinitely large random matrices. We present results for the average IPR as a function of the eigenvalue and the presence of a localization transition for Laplacian matrices on a sparse random graph and for fully-connected Lévy matrices. In the case of Lévy matrices, we calculate a critical line that separates localized from extended eigenstates. The theoretical results for $N \rightarrow \infty$ are compared with numerical diagonalization of finite matrices and with results of previous works.

In the next section we define the average quantities of interest and we discuss how they can be calculated in the limit $N \rightarrow \infty$. The results for the average IPR and the localization transition in the case of Laplacian and Lévy matrices are shown in section III. In section

IV we present our conclusions. An equation that relates the Green function and the IPR is derived in appendix A. We include a detailed discussion of the cavity method for the ensemble of Lévy matrices in appendix B.

II. THE GENERAL SETTING

In this section we show how the DOS and the IPR are written in terms of the diagonal elements of the Green function. The joint distribution of the real and imaginary parts of these diagonal elements is the central quantity of interest to determine the average DOS and IPR. We discuss how the cavity method can be employed in order to calculate this distribution in the large N limit.

A. Random matrix parameters

We define an ensemble Ω_N of symmetric $N \times N$ random matrices with real elements. Assuming that a given matrix $\mathbf{J} \in \Omega_N$ has a set of eigenvalues $\{\lambda_\mu\}_{\mu=1,\dots,N}$ and normalized eigenvectors $\{| \mu \rangle\}_{\mu=1,\dots,N}$, the DOS lying between λ and $\lambda + d\lambda$ is given by

$$\rho(\lambda) = \lim_{N \rightarrow \infty} \frac{1}{N} \sum_{\mu=1}^N \delta(\lambda - \lambda_\mu). \quad (1)$$

The IPR associated to a given eigenvector $| \mu \rangle$ is defined as

$$Y_\mu^N = \sum_{i=1}^N (\psi_\mu^i)^4, \quad (2)$$

where $\psi_\mu^i = \langle i | \mu \rangle$ is the component i of the eigenvector $| \mu \rangle$. The set of normalized vectors $\{| i \rangle\}_{i=1,\dots,N}$ is the canonical site basis. The IPR allows one to distinguish between two extreme situations in the limit $N \rightarrow \infty$. In a delocalized or extended region of the spectrum, a number of sites of $O(N)$ contributes to a given eigenstate. Due to the normalization $\sum_{i=1}^N (\psi_\mu^i)^2 = 1$, the components of a given $| \mu \rangle$ satisfy $\psi_\mu^i = O(1/\sqrt{N})$ and, as a consequence, we have $\lim_{N \rightarrow \infty} Y_\mu^N = 0$. In contrast, only a finite number of components $\{\psi_\mu^i\}$ is nonzero for a localized eigenstate. The components of a state μ localized on d sites satisfy $\psi_\mu^i = O(1/\sqrt{d})$ and the IPR is given by $Y_\mu^N = O(1/d)$ in the limit $N \rightarrow \infty$. This simple analysis shows that the IPR is a suitable parameter for a quantitative description of the transition between extended and localized eigenstates.

Here we are interested in the average behaviour of Y_μ^N over all the states in an infinitesimal region of the spectrum. We define the eigenvalue dependent IPR

$$P(\lambda) = \lim_{N \rightarrow \infty} \frac{1}{N\rho(\lambda)} \sum_{\mu=1}^N \delta(\lambda - \lambda_\mu) Y_\mu^N, \quad (3)$$

which is the limit $N \rightarrow \infty$ of the average value of Y_μ^N over all the states lying between λ and $\lambda + d\lambda$ when $\rho(\lambda)$ is finite.

The quantity that allows one to determine the DOS and the IPR is the Green function associated to \mathbf{J} . Its diagonal elements are defined as follows

$$G_{ii}^N(z) = (z - \mathbf{J})_{ii}^{-1} = \sum_{\mu=1}^N \frac{(\psi_\mu^i)^2}{z - \lambda_\mu}, \quad (4)$$

where z is the complex variable $z = \lambda - i\epsilon$. The DOS can be obtained in the limit $\epsilon \rightarrow 0^+$ according to

$$\rho(\lambda) = \lim_{\epsilon \rightarrow 0^+} \lim_{N \rightarrow \infty} \frac{1}{\pi N} \sum_{j=1}^N \text{Im} G_{jj}^N(\lambda - i\epsilon). \quad (5)$$

The IPR is expressed by

$$P(\lambda) = \lim_{\epsilon \rightarrow 0^+} \lim_{N \rightarrow \infty} \frac{\epsilon}{\pi N \rho(\lambda)} \sum_{j=1}^N |G_{jj}^N(\lambda - i\epsilon)|^2 \quad (6)$$

in the regions of the spectrum where there are no degenerate states. Equation (6) has been employed in the study of localization properties through the supersymmetric approach [23]. In appendix A we explain how to derive eq. (6). Finally, we rewrite eqs. (5) and (6) as follows

$$\rho(\lambda) = \lim_{\epsilon \rightarrow 0^+} \frac{1}{\pi} \langle \text{Im} \omega \rangle, \quad (7)$$

$$P(\lambda) = \frac{1}{\pi \rho(\lambda)} \lim_{\epsilon \rightarrow 0^+} \epsilon \langle |\omega|^2 \rangle, \quad (8)$$

where we have introduced the average $\langle f(\omega) \rangle = \int d\omega W_{\lambda,\epsilon}(\omega) f(\omega)$ with respect to the joint distribution $W_{\lambda,\epsilon}(\omega)$ of the real and imaginary parts of $G_{ii}^N(z)$

$$W_{\lambda,\epsilon}(\omega) = \lim_{N \rightarrow \infty} \frac{1}{N} \sum_{j=1}^N \langle \delta[\omega - G_{jj}^N(\lambda - i\epsilon)] \rangle_{\mathbf{J}}. \quad (9)$$

We have assumed that the distribution of $G_{ii}^N(z)$ is a self-averaging quantity in the limit $N \rightarrow \infty$, with $\langle \dots \rangle_{\mathbf{J}}$ denoting the ensemble average with respect to the distribution of \mathbf{J} . This implies that $\rho(\lambda)$ and $P(\lambda)$ are self-averaging quantities in the limit $N \rightarrow \infty$. The integrals present in $\langle f(\omega) \rangle$ run over the entire real and imaginary axes of ω . Our goal consists in calculating the distribution $W_{\lambda,\epsilon}(\omega)$, since this quantity allows us to compute the average DOS and IPR through eqs. (7) and (8).

B. A cavity calculation of the distribution of Green functions

In this subsection we explain how the cavity method can be used in order to calculate $W_{\lambda,\epsilon}(\omega)$. As an example, the technical details involved in the calculations are

shown in appendix B for the case of fully-connected Lévy matrices.

The diagonal elements of the Green function can be written as a Gaussian integral over the real vectors $\mathbf{x} = (x_1, \dots, x_N)$, namely

$$G_{kk}^N(z) = i \frac{\int d\mathbf{x} x_k^2 \exp \left[-\frac{i}{2} \sum_{ij=1}^N x_i (z - \mathbf{J})_{ij} x_j \right]}{\int d\mathbf{x} \exp \left[-\frac{i}{2} \sum_{ij=1}^N x_i (z - \mathbf{J})_{ij} x_j \right]}. \quad (10)$$

Defining the normalized complex function

$$\mathcal{P}_{N,z}(\mathbf{x}) = \frac{\exp[-H_{N,z}(\mathbf{x})]}{\int d\mathbf{x} \exp[-H_{N,z}(\mathbf{x})]}, \quad (11)$$

with

$$H_{N,z}(\mathbf{x}) = \frac{i}{2} \sum_{ij=1}^N x_i (z - \mathbf{J})_{ij} x_j, \quad (12)$$

the elements $G_{kk}^N(z)$ assume the form

$$G_{kk}^N(z) = i \int d\mathbf{x} x_k^2 \mathcal{P}_{N,z}(\mathbf{x}) = i \int dx_k x_k^2 \mathcal{P}_{N,z}(x_k), \quad (13)$$

where $\mathcal{P}_{N,z}(x_k)$ follows from $\mathcal{P}_{N,z}(\mathbf{x})$ by integrating over all variables besides x_k . More generally, we write for a set A of indices

$$\mathcal{P}_{N,z}(x_A) = \int \left[\prod_{i \notin A} dx_i \right] \mathcal{P}_{N,z}(\mathbf{x}). \quad (14)$$

Equation (13) shows that the Green functions $\{G_{kk}^N(z)\}$ can be computed for a single instance of \mathbf{J} once we know how to calculate the local marginals $\{\mathcal{P}_{N,z}(x_k)\}$.

Disordered spin models on a random graph are defined through a probability measure on this graph. The cavity method provides an efficient way to compute the local marginals of disordered spin systems defined on fully-connected [31] and finitely connected random graphs [30]. The application of the cavity method to the study of random matrices relies on the analogy between the random matrix problem and disordered spin systems defined on graphs [13]. Using this similarity one can apply the cavity method to calculate the marginals $\{\mathcal{P}_{N,z}(x_k)\}$.

One can associate a random graph to a random matrix as follows: the graph contains N nodes. A certain variable x_i ($i = 1, \dots, N$) is associated to the corresponding node i of the graph. When $J_{ij} = 0$ there is no edge between nodes i and j , while this pair of nodes is connected when $J_{ij} \neq 0$. The interaction strength between nodes i and j is given by the value of J_{ij} , such that \mathbf{J} specifies the topology of the random graph and the interaction strengths between the nodes.

For a given graph instance \mathcal{G} , ∂_i is the set of nodes connected to a certain node i . The cavity method is based on the assumption that the distribution $\mathcal{P}_{N,z}(\mathbf{x}_{\partial_i})$

of the variables in the neighbourhood ∂_i factorizes on the cavity graph $G^{(i)}$, i.e.

$$\mathcal{P}_{N,z}^{(i)}(\mathbf{x}_{\partial_i}) = \prod_{j \in \partial_i} \mathcal{P}_{N,z}^{(i)}(x_j). \quad (15)$$

The cavity graph $G^{(i)}$ is the subgraph of G where node i and all its connections have been removed. The marginals $\{\mathcal{P}_{N,z}^{(i)}(x_i)\}$ are defined on the cavity graph. Since the local marginals $\{\mathcal{P}_{N,z}(x_j)\}$ on the real graph can be written in terms of the local marginals on $\mathcal{G}^{(i)}$, one can solve first the problem on the cavity graph as a function of $\{\mathcal{P}_{N,z}^{(i)}(x_j)\}$ and then reconstruct the local marginals $\{\mathcal{P}_{N,z}(x_j)\}$.

In the case of disordered spin systems defined on finitely connected graphs, the cavity method is also known as the Bethe-Peierls iterative method [30]. In this case, we expect that the factorization assumption (15) holds outside the spin-glass phase since the graph looks locally like a tree. When the graph is a tree the condition (15) holds for $N \rightarrow \infty$. In the case of disordered spin systems defined on fully-connected graphs, the vanishing of the connected correlation functions for $N \rightarrow \infty$ ensures that the assumption (15) holds outside the spin-glass phase [31].

By employing the cavity method and following analogous calculations as done in [13], we show in appendix B that the marginal $\mathcal{P}_{N,z}(x_k)$ at site k is given by

$$\mathcal{P}_{N,z}(x_k) = \sqrt{\frac{i}{2\pi G_{kk}^N(z)}} \exp\left(-\frac{i x_k^2}{2G_{kk}^N(z)}\right). \quad (16)$$

The diagonal elements of the Green function are determined from the fixed-point solution of the equations

$$G_{ii}^{N,(k)}(z) = \frac{1}{z - \sum_{j \in \partial_i \setminus k} h_{ij}^N(J_{ij}, G_{jj}^{N,(i)}(z))}, \quad (17)$$

$$G_{ii}^N(z) = \frac{1}{z - \sum_{j \in \partial_i} h_{ij}^N(J_{ij}, G_{jj}^{N,(i)}(z))}, \quad (18)$$

for $i = 1, \dots, N$ and for all $k \in \partial_i$, where ∂_i is the set of all indices j in a given row i such that $J_{ij} \neq 0$. The symbol $\partial_i \setminus k$ denotes the set ∂_i without index k . The quantities $\{G_{ii}^{N,(k)}(z)\}$ are the diagonal elements of the Green function of the matrix following from the original matrix through removal of row k and column k . The specificity of the random matrices under study can manifest itself only in the number of indices present in ∂_i and in the form of the function $h_{ij}^N(J_{ij}, G_{jj}^{N,(i)}(z))$.

For fully-connected Lévy matrices and Laplacian matrices considered in this work, $h_{ij}^N(J_{ij}, G_{jj}^{N,(i)}(z))$ assumes the form:

- Lévy matrices:

$$h_{ij}^N(J_{ij}, G_{jj}^{N,(i)}(z)) = J_{ij}^2 G_{jj}^{N,(i)}(z), \quad (19)$$

- Laplacian matrices:

$$h_{ij}^N(J_{ij}, G_{jj}^{N,(i)}(z)) = \frac{J_{ij}^2 G_{jj}^{N,(i)}(z)}{1 + J_{ij} G_{jj}^{N,(i)}(z)} - J_{ij} . \quad (20)$$

Equations (17) and (18) with $h_{ij}^N(J_{ij}, G_{jj}^{N,(i)}(z))$ given by (19) have been obtained previously in the study of fully-connected Lévy matrices [20] and sparse random matrices [13].

A self-consistent equation for $W_{\lambda,\epsilon}(\omega)$ is obtained by substituting eq. (18) in eq. (9) and performing the average over the ensemble of random matrices. We have solved numerically this self-consistent equation through a population dynamics algorithm [30], which consists in parametrizing the distribution $W_{\lambda,\epsilon}(\omega)$ by a large population of stochastic variables representing instances of ω . At each iteration step, one of these variables is chosen at random and updated according to its probability distribution, until a stationary form for $W_{\lambda,\epsilon}(\omega)$ is reached. A detailed discussion of the population dynamics method in the context of random matrices and the corresponding algorithm are presented in [14].

According to eqs. (7) and (8), one has to obtain numerical results for the distribution $W_{\lambda,\epsilon}(\omega)$ in the limit $\epsilon \rightarrow 0$. One has to calculate $W_{\lambda,\epsilon}(\omega)$ for very small but finite values of ϵ , since Dirac delta peaks might arise, for instance, in the spectrum of sparse random matrices. In this way the Dirac delta peaks are approximated by Lorentzian functions with a finite width ϵ [13, 14]. In the next section, we specify the ensembles of random matrices and the corresponding distribution $W_{\lambda,\epsilon}(\omega)$ for each case.

III. RESULTS

In this section we show the results for two different ensembles of symmetric random matrices: Laplacian matrices on sparse random graphs and fully-connected Lévy matrices. In both cases we focus on the behaviour of the average IPR and the presence of a localization transition.

A. Laplacian matrices

The elements of the Laplacian matrix \mathbf{J} on a random graph can be defined according to [14]

$$J_{ij} = c_{ij} K_{ij} - \delta_{ij} \sum_{k=1}^N c_{ik} K_{ik} , \quad (21)$$

in which \mathbf{c} and \mathbf{K} are symmetric matrices. We consider here only the case in which the elements of the connectivity matrix \mathbf{c} are i.i.d.r.v drawn from the distribution

$$p_c(c_{ij}) = \left(1 - \frac{c}{N}\right) \delta_{c_{ij},0} + \frac{c}{N} \delta_{c_{ij},1} , \quad (22)$$

with $c_{ii} = 0$ for $\forall i$. In the limit $N \rightarrow \infty$, \mathbf{J} has a sparse structure and the number of nonzero elements per row exhibits a Poissonian distribution with average c . The nonzero elements $\{K_{ij}\}$ are drawn according to the distribution $p_K(K_{ij})$. We consider here two different cases: (i) the elements $\{K_{ij}\}$ assume a fixed value $K_{ij} = -1/c$, such that $p_K(K_{ij}) = \delta(K_{ij} + 1/c)$; (ii) the elements $\{K_{ij}\}$ are drawn from a Gaussian distribution with zero mean and variance $1/c$.

Inserting eq. (18) in eq. (9) and performing the ensemble average, one can derive the following self-consistent equation for $W_{\lambda,\epsilon}(\omega)$

$$W_{\lambda,\epsilon}(\omega) = \sum_{k=0}^{\infty} \frac{e^{-c} c^k}{k!} \int \left[\prod_{l=1}^k d\omega_l W_{\lambda,\epsilon}(\omega_l) \right] \times \int \left[\prod_{l=1}^k dK_l p_K(K_l) \right] \delta \left(\omega - \frac{1}{z - \sum_{l=1}^k H(\omega_l, K_l)} \right) . \quad (23)$$

The updating function $H(\omega, K)$ is given by

$$H(\omega, K) = \frac{K^2 \omega}{1 + K \omega} - K . \quad (24)$$

The population dynamics algorithm can be used to solve eq. (23) numerically [30].

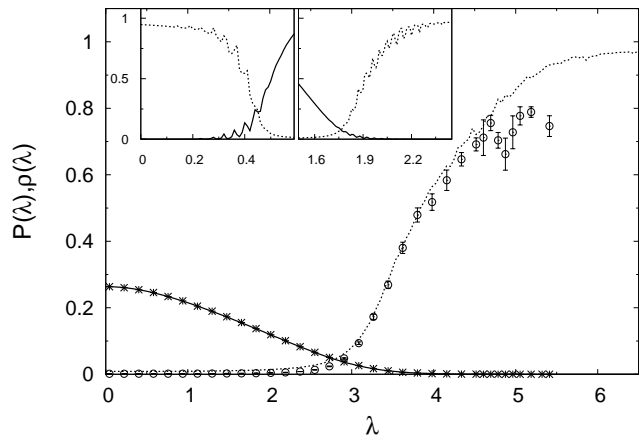


FIG. 1: Population dynamics results for the average DOS (solid lines) and IPR (dotted lines) for Laplacian matrices with $c = 20$ and elements $\{K_l\}$ drawn from a Gaussian distribution. These results were obtained with $\epsilon = 0.001$ and a population of 5×10^6 samples for the distribution $W_{\lambda,\epsilon}(\omega)$. Numerical diagonalization results for the DOS (*) and the IPR (o) obtained with an ensemble of 500 matrices of dimension $N = 3000$ are shown. Error bars for the IPR are indicated. The insets show population dynamics results for the DOS (solid lines) and the IPR (dotted lines) as a function of λ in the left and right tails of the spectrum of Laplacian matrices with $c = 20$, $\epsilon = 0.001$ and fixed elements $\{K_l\}$.

In fig. 1 we illustrate the results for $\rho(\lambda)$ and $P(\lambda)$ obtained from the population dynamics algorithm and from

diagonalization of finite matrices for $c = 20$. The spectra of random matrices with a sparse structure contain delta peaks located at the eigenvalues of isolated finite-size clusters for any value of c [11, 13, 14]. Eq. (6) gives an approximation for the IPR in these regions of the spectrum due to the presence of degenerate states. In order to minimize the effect of these singular contributions, we have chosen a large value of c . The main graph of fig. 1 illustrates $\rho(\lambda)$ and $P(\lambda)$ for the Gaussian distribution of $\{K_l\}$ only when $\lambda \geq 0$, since the spectrum is symmetric around zero. The insets show the behaviour of $\rho(\lambda)$ and $P(\lambda)$ in the tails of the spectrum for the case of fixed $K_l = -1/c$. In both cases, $P(\lambda)$ is vanishingly small in the central part of the spectrum, corresponding to a region of extended eigenstates. The eigenvectors undergo a localization transition in the tails of the spectrum, as shown by the increase of $P(\lambda)$. It is difficult to determine the IPR through numerical diagonalization in the tails of the spectrum since one has to diagonalize extremely large matrices.

By means of numerical diagonalization and a single defect approximation (SDA) [12, 16], the authors of [16] have studied the eigenstates corresponding to the regular peaks that appear for large and small eigenvalues in the spectrum of Laplacian matrices with fixed values of $\{K_l\}$. They have found that these states are localized on a finite number of sites that have a small or large connectivity in comparison to the mean c . Fig. 1 complements these results by showing that $P(\lambda) \rightarrow 1$ for large values of λ , which means that eigenstates corresponding to large eigenvalues are localized on a single site. The presence of the peaks is reduced when one introduces Gaussian disorder in the elements $\{K_l\}$.

The agreement between diagonalization and theoretical results for $\rho(\lambda)$ in fig. 1 is very good. We have found that $\rho(\lambda)$ depends weakly on N or ϵ in the case of numerical diagonalization or population dynamics, respectively. In the case of $P(\lambda)$, both results exhibit a very good agreement in the central region of the spectrum and in parts of the tails, for the particular values of ϵ and N chosen. The results show a discrepancy in the far regions of the tails where the eigenvalues are rare, as shown by the higher fluctuations in the numerical diagonalization, illustrated by the error bars. However, the average IPR depends on the values of N and ϵ .

Figure 2 illustrates the behaviour of $P(\lambda)$ as a function of N and ϵ for the Laplacian matrix with Gaussian elements $\{K_l\}$ and $c = 20$. The results show that, for $\lambda = 2.90$ and $\lambda = 3.35$, the average IPR goes to zero when $\epsilon \rightarrow 0$. Accordingly, the diagonalization results for $P(\lambda)$ exhibit a similar qualitative behaviour as N increases. For $\lambda = 6.70$, the average IPR has a finite value for $\epsilon \rightarrow 0$, since this is the region of localized eigenstates. These results indicate that the localization transition presented in fig. 1 becomes sharper for $N \rightarrow \infty$. By employing numerical diagonalization methods, the authors of [16] have found the value $\lambda_c \simeq 1.67$ for the mobility edge on the right tail in the case of Laplacian matrices

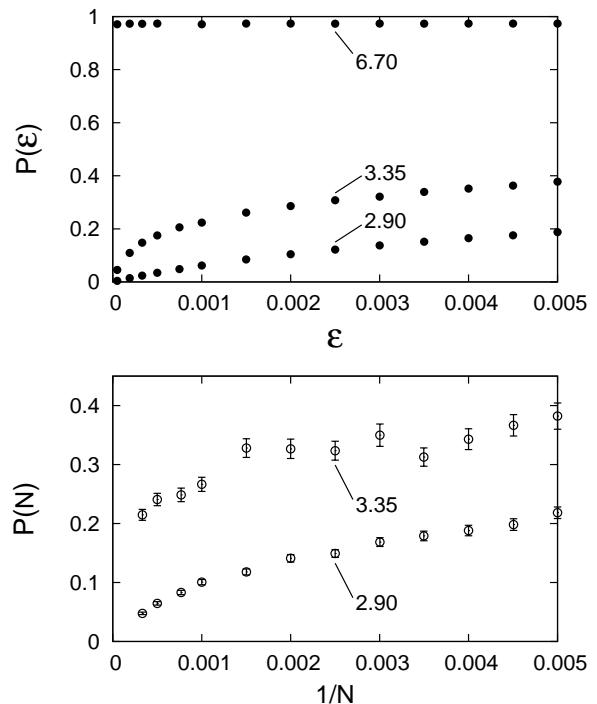


FIG. 2: Average IPR for Laplacian matrices as a function of ϵ (population dynamics, top graph) and N (numerical diagonalization, bottom graph) for $c = 20$ and different numerical values of λ , which are shown explicitly on the figure. The elements $\{K_l\}$ are drawn from the Gaussian distribution described in the text. The diagonalization results were obtained considering an ensemble of 500 matrices for each N , with error bars included in this case. The population dynamics results were obtained with a population of 5×10^6 samples.

with $c = 20$ and fixed elements $\{K_l\}$. We have calculated approximately the localization threshold λ_c on the right tail by using the ϵ independence of $P(\lambda)$ as a criterion to determine the localized region. For $c = 20$ we have found the values $\lambda_c \simeq 1.95$ and $\lambda_c \simeq 5.65$ for Laplacian matrices with fixed and Gaussian elements $\{K_l\}$, respectively.

B. Lévy matrices

The fully-connected Lévy matrix is a symmetric matrix in which $J_{ii} = 0$ for $\forall i$. The nondiagonal elements are i.i.d.r.v. drawn from the Lévy distribution $P_\alpha(J)$, defined through the characteristic function $L_\alpha(q)$

$$P_\alpha(J) \equiv \int \frac{dq}{2\pi} \exp(-iqJ) L_\alpha(q). \quad (25)$$

The characteristic function is of the form

$$\ln L_\alpha(q) = - \left| \frac{q}{\sqrt{2}N^{1/\alpha}} \right|^\alpha. \quad (26)$$

The distribution $P_\alpha(J)$ is fully determined by the parameter $\alpha \in (0, 2]$. For $\alpha < 2$, α characterizes the power-law

decay of $P_\alpha(J)$. We consider only Lévy distributions centered around zero. The scaling with N in eq. (26) ensures that the spectrum converges to a stable form in the limit $N \rightarrow \infty$ [20]. The distribution of Green functions does not depend on the skewness parameter [20, 22].

For $\alpha = 2$ we recover the Gaussian orthogonal ensemble since $P_\alpha(J)$ is a Gaussian distribution with zero mean and variance $1/N$. For $\alpha < 2$, the asymptotic behaviour of $P_\alpha(J)$ for $|J| \rightarrow \infty$ can be derived from the explicit form of $L_\alpha(q)$:

$$\lim_{|J| \rightarrow \infty} P_\alpha(J) = \frac{C_\alpha}{N|J|^{\alpha+1}}, \quad (27)$$

where

$$C_\alpha = \left(\frac{1}{\sqrt{2}}\right)^\alpha \frac{1}{\pi} \sin\left(\frac{\alpha\pi}{2}\right) \Gamma(\alpha+1). \quad (28)$$

The integrals for the second and higher moments of the distribution diverge for $\alpha < 2$ due to the power-law decay illustrated by eq. (27).

Due to the power-law tails of the Lévy distribution, each row of \mathbf{J} contains an infinite number of elements of order $O(N^{-1/\alpha})$ and a finite number of elements of order $O(1)$. For small values of α , it has been argued that fully-connected Lévy matrices can be seen as sparse random matrices [20, 21]. The spectrum of Lévy matrices has been calculated with the cavity method in previous works [20, 22] and an equation for the distribution of Green functions has been determined using the generalized central limit theorem [32]. We have followed a different approach to calculate the distribution of Green functions, in which the underlying sparse character of Lévy matrices becomes transparent. Besides that, the resulting self-consistent equation can be solved through a population dynamics algorithm, which is a practical advantage in comparison with previous works where one has to deal with a complicated system of integral equations [22].

In order to take the ensemble average and the limit $N \rightarrow \infty$ of the distribution of Green functions, we introduce a cutoff γ that makes an explicit distinction between strong matrix elements $J_{ij} > \gamma$ and weak matrix elements $J_{ij} < \gamma$ (see appendix B). This trick has been introduced in spin systems in [33, 34] The backbone of strong matrix elements can be treated as a sparse random matrix, leading to the following self-consistent equation

$$\begin{aligned} W_{\lambda,\epsilon,\gamma}(\omega) &= \sum_{k=0}^{\infty} \frac{e^{-c_\gamma} c_\gamma^k}{k!} \int \left[\prod_{l=1}^k d\omega_l W_{\lambda,\epsilon,\gamma}(\omega_l) \right] \\ &\times \int \left[\prod_{l=1}^k dJ_l p_{J,\gamma}(J_l) \right] \\ &\times \delta \left(\omega - \frac{1}{z - \sigma_\gamma^2 \langle \omega \rangle - \sum_{l=1}^k H(\omega_l, J_l)} \right), \quad (29) \end{aligned}$$

where

$$H(\omega, J) = J^2 \omega \quad (30)$$

$$p_{J,\gamma}(J) = \begin{cases} \frac{\alpha \gamma^\alpha}{2|J|^{\alpha+1}} & |J| > \gamma \\ 0 & |J| < \gamma \end{cases}, \quad (31)$$

and

$$c_\gamma = \frac{2C_\alpha}{\alpha \gamma^\alpha}, \quad (32)$$

$$\sigma_\gamma^2 = \frac{2\gamma^{2-\alpha} C_\alpha}{2-\alpha}. \quad (33)$$

The distribution of Green functions follows from $W_{\lambda,\epsilon}(\omega) = \lim_{\gamma \rightarrow 0} W_{\lambda,\epsilon,\gamma}(\omega)$.

The quantity c_γ is the average number of strong matrix elements per row and $p_{J,\gamma}(J)$ denotes their distribution. The contribution of the infinite number of weak matrix elements is taken into account through the law of large numbers, leading to a term proportional to their variance σ_γ^2 . Eq. (29) shows that the distribution $W_{\lambda,\epsilon,\gamma}(\omega)$ contains a part coming from a sparse random matrix of strong matrix elements and an average contribution due to the weak matrix elements.

We have solved eq. (29) through a population dynamics algorithm. The idea is to obtain results for small values of the cutoff γ . In fig. 3 we show results for the DOS of Lévy matrices obtained from the numerical diagonalization of finite matrices and from the numerical solution of eq. (29). The DOS of Lévy matrices is symmetric around zero. For both values of α the agreement between diagonalization and population dynamics results is excellent.

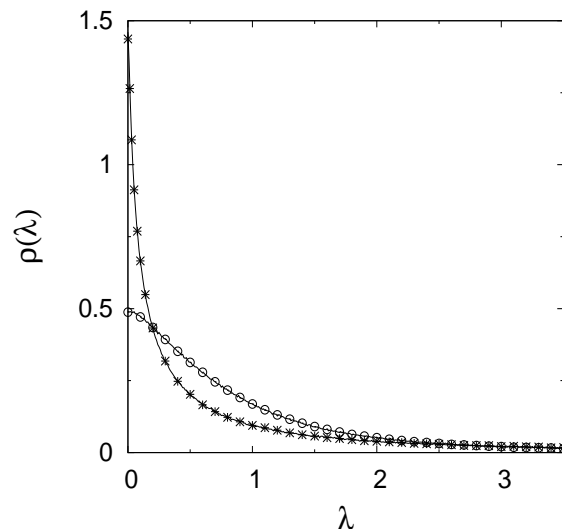


FIG. 3: Comparison between numerical diagonalization (full lines) and population dynamics results (different types of symbols) for the average DOS of Lévy matrices with $\alpha = 0.75$ (*) and $\alpha = 1.25$ (o). The diagonalization results were obtained considering an ensemble of 1000 matrices of dimension $N = 1500$. The population dynamics results were obtained considering $\epsilon = 0.001$, $\gamma = 0.01$ and a population of 10^6 samples.

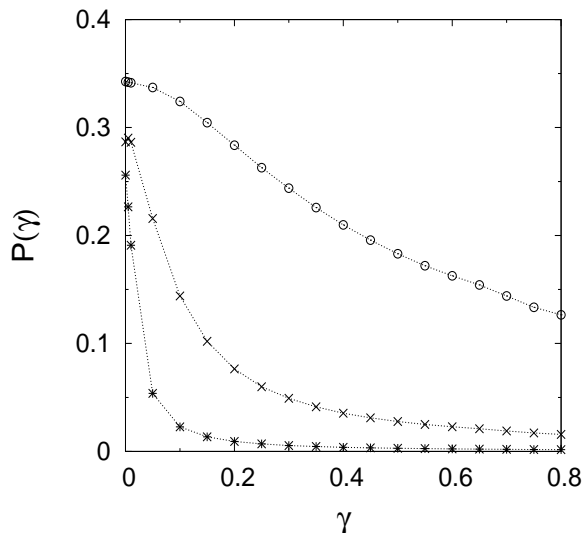


FIG. 4: Population dynamics results for the average IPR of Lévy matrices as a function of γ for $\alpha = 0.5$, $\lambda = 1$ and a population of 5×10^6 samples. Three different values of ϵ are shown: $\epsilon = 0.01$ (\circ), $\epsilon = 0.001$ (\times) and $\epsilon = 0.0001$ ($*$). The average IPR depends on ϵ for $\gamma \rightarrow 0$.

For $\alpha \rightarrow 2$, we obtain $c_\gamma \rightarrow 0$ and $\sigma_\gamma^2 \rightarrow 1$, and the distribution $W_{\lambda,\epsilon,\gamma}(\omega)$ reduces to the simple form

$$W_{\lambda,\epsilon}(\omega) = \delta\left(\omega - \frac{1}{z - \langle\omega\rangle}\right). \quad (34)$$

When inserted in the definition of $\langle\omega\rangle$, eq. (34) gives rise to a quadratic equation for $\langle\omega\rangle$ whose solution leads to the Wigner semicircle law by means of eq. (7).

In figs. 4 and 5 we illustrate the population dynamics results for the behaviour of $P(\gamma)$ as a function of γ for $\lambda = 1$ and $\lambda = 5$, respectively. In both figures we consider $\alpha = 0.5$ and three different values of ϵ . Figure 4 shows that for $\gamma \rightarrow 0$ the average IPR decreases for decreasing values of ϵ , which is an indication that $\lambda = 1$ corresponds to a region with delocalized states. As γ decreases in fig. 5, $P(\gamma)$ converges to a finite value that does not depend on ϵ , which corresponds to a region of localized states.

We have used the ϵ independence of $P(\lambda)$ in the localized region as a criterion to calculate approximately the localization threshold in the limit $N \rightarrow \infty$. In fig. 6 we present results for the critical line separating localized from extended states in the (α, λ) plane for $\gamma = 0.008$. For small values of α , c_γ is small and the tails of the distribution $p_{J,\gamma}(J)$ are very long. In this case the sparse matrix character of Lévy matrices is highlighted and the region of localized eigenstates is larger. For increasing values of α , the parameter c_γ increases and the tails of the distribution $p_{J,\gamma}(J)$ are less long. The distinction between strong and weak matrix elements becomes less important and the fully-connected character of Lévy matrices is highlighted, leading to a larger region of extended eigenstates. The results for the localization transition when α is large are very noisy due to the larger values of λ_c involved in the calculations. This makes the results

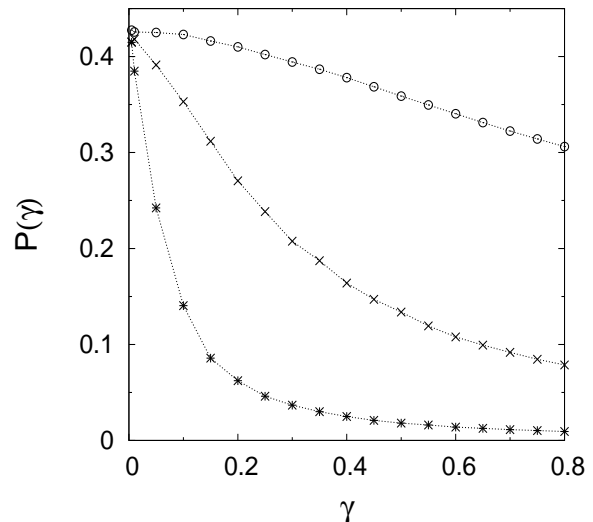


FIG. 5: Population dynamics results for the average IPR of Lévy matrices as a function of γ for $\alpha = 0.5$, $\lambda = 5$ and a population of 5×10^6 samples. Three different values of ϵ are shown: $\epsilon = 0.01$ (\circ), $\epsilon = 0.001$ (\times) and $\epsilon = 0.0001$ ($*$). The average IPR is independent of ϵ for $\gamma \rightarrow 0$.

for $\alpha > 1.3$ very inaccurate. Besides that, the population dynamics algorithm becomes slower for increasing values of c_γ . We have obtained numerically that the average number of strong matrix elements c_γ reaches its maximum value at $\alpha \simeq 2$ when $\gamma \rightarrow 0$. This indicates that the region of extended states is the largest possible for $\alpha \simeq 2$.

For $\alpha = 0.5$ the population dynamics results show that $P(\lambda) \rightarrow 1/2$ as $\lambda \rightarrow \infty$. This result agrees with the discussion presented in [20]. According to this work, due to the strong fluctuations of the Lévy matrix elements, the eigenstates corresponding to large eigenvalues are localized on pairs of very strongly interacting sites, which leads to an IPR equal to $1/2$. Based mostly on numerical diagonalization results [20, 21], previous works point to the presence of three regions: a region of extended eigenstates, a strictly localized region, with exponentially localized eigenstates, and a mixed region, exhibiting both localized and extended features. The results of the literature [20] suggest that the eigenstates decay algebraically in the mixed region. From the study of the IPR one can not distinguish between these two different types of localized states.

IV. CONCLUSION

In this paper we have studied the localization of eigenvectors of random matrices through the calculation of the inverse participation ratio with the cavity method. We have found a self-consistent equation for the inverse participation ratio in the limit $N \rightarrow \infty$, which can be solved numerically through a population dynamics algorithm.

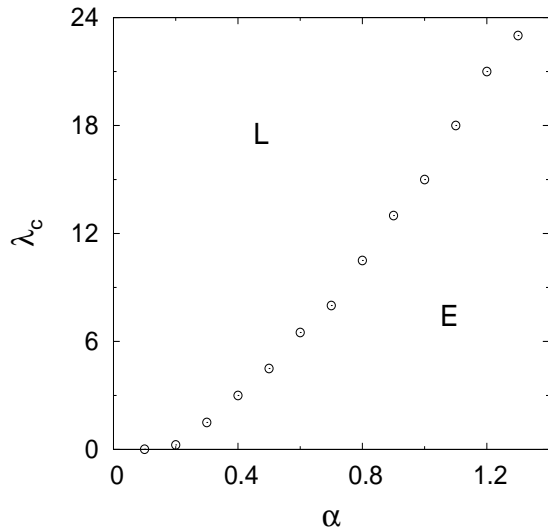


FIG. 6: Population dynamics results for the critical line separating localized (L) from extended states (E) in the fully-connected Lévy matrix. The results were obtained considering $\epsilon = 0.0001$, $\gamma = 0.008$ and a population of 10^6 samples.

Therefore, this approach contains no finite size effects in contrast with numerical diagonalization methods. The resultant equations for the inverse participation ratio are conjectured to be exact for Laplacian matrices on sparse random graphs and for fully connected Lévy matrices in the limit $N \rightarrow \infty$.

We have calculated the inverse participation ratio of Laplacian matrices on sparse random graphs. The spectrum is characterized by a delocalized part centered around zero and a localized part in the edges of the spectrum. The states corresponding to large eigenvalues are localized on single sites with large degrees in comparison to the average connectivity [16]. Numerical diagonalization results for the inverse participation ratio appear to converge to the corresponding theoretical values for $N \rightarrow \infty$ when there is no degeneracy in the eigenvalues.

The matrix elements of random Lévy matrices are drawn from a distribution with power-law tails characterized by an exponent α . In previous works [20, 21], the localization properties of Lévy matrices have been studied using mainly diagonalization results. These results indicate that the eigenstates of Lévy matrices undergo a transition from a delocalized to a localized phase. However, large finite size effects are present in such calculations. Using the cavity approach we have determined a transition line separating localized from delocalized states in the (α, λ) plane by studying the behaviour of the inverse participation ratio in the limit $N \rightarrow \infty$. Our results confirm the presence of a region with localized states for large eigenvalues, where the states are localized on pairs of very strongly interacting sites [20].

While we were writing this paper a preprint appeared on the arxiv addressing similar issues [35]. The authors of this paper have determined the location of the An-

person transition in electronic systems on Bethe lattices using the cavity method, while we have focused on the localization properties of random matrix ensembles.

Appendix A: The eigenvalue-dependent IPR and the Green function

In this appendix we show how the eigenvalue-dependent IPR can be expressed in terms of $G_{ii}^N(\lambda - i\epsilon)$ by means of eq. (6). By substituting eq. (4), one can write down the following quantity

$$\mathcal{G}_j^N(\lambda) = \lim_{\epsilon \rightarrow 0} \epsilon |G_{jj}^N(\lambda - i\epsilon)|^2, \quad (\text{A1})$$

in the form

$$\mathcal{G}_j^N(\lambda) = \lim_{\epsilon \rightarrow 0} \epsilon \sum_{\mu=1}^N \frac{(\psi_{\mu}^j)^4}{(\lambda - \lambda_{\mu})^2 + \epsilon^2} + \lim_{\epsilon \rightarrow 0} D_j^N(\epsilon, \lambda), \quad (\text{A2})$$

where we have defined the non-diagonal contribution

$$D_j^N(\epsilon, \lambda) = \epsilon \sum_{\mu=1}^N \frac{(\psi_{\mu}^j)^2}{\lambda - \lambda_{\mu} + i\epsilon} \sum_{\nu \neq \mu} \frac{(\psi_{\nu}^j)^2}{\lambda - \lambda_{\nu} - i\epsilon}. \quad (\text{A3})$$

Assuming there is a set of eigenvalues $\mathcal{A} = \{\lambda_{k_1}, \dots, \lambda_{k_K}\}$ such that $\lambda = \lambda_{k_i}$ for any $\lambda_{k_i} \in \mathcal{A}$, we can rewrite $D_i^N(\epsilon, \lambda)$ as follows

$$\begin{aligned} D_i^N(\epsilon, \lambda) &= \frac{1}{i} \sum_{j=1}^K (\psi_{k_j}^j)^2 \sum_{\nu \neq k_j} \frac{(\psi_{\nu}^j)^2}{\lambda - \lambda_{\nu} - i\epsilon} \\ &\quad - \frac{1}{i} \sum_{j=1}^K (\psi_{k_j}^l)^2 \sum_{\nu \neq \mathcal{A}} \frac{(\psi_{\nu}^l)^2}{\lambda - \lambda_{\nu} + i\epsilon} \\ &\quad + \epsilon \sum_{\mu \neq \mathcal{A}} \frac{(\psi_{\mu}^l)^2}{\lambda - \lambda_{\mu} + i\epsilon} \sum_{\nu \neq \mu, \mathcal{A}} \frac{(\psi_{\nu}^l)^2}{\lambda - \lambda_{\nu} - i\epsilon}. \end{aligned} \quad (\text{A4})$$

In the absence of degenerate states in the spectrum, the set \mathcal{A} is simply given by $\mathcal{A} = \lambda_k$, which reads

$$\begin{aligned} D_j^N(\epsilon, \lambda) &= \frac{1}{i} (\psi_k^j)^2 \sum_{\nu \neq k} \frac{(\psi_{\nu}^j)^2}{\lambda - \lambda_{\nu} - i\epsilon} \\ &\quad - \frac{1}{i} (\psi_k^j)^2 \sum_{\nu \neq k} \frac{(\psi_{\nu}^j)^2}{\lambda - \lambda_{\nu} + i\epsilon} \\ &\quad + \epsilon \sum_{\mu \neq k} \frac{(\psi_{\mu}^j)^2}{\lambda - \lambda_{\mu} + i\epsilon} \sum_{\nu \neq \mu, k} \frac{(\psi_{\nu}^j)^2}{\lambda - \lambda_{\nu} - i\epsilon}. \end{aligned} \quad (\text{A5})$$

Thus we obtain $\lim_{\epsilon \rightarrow 0} D_i^N(\epsilon, \lambda) = 0$ and eq. (A2) assumes the form

$$\mathcal{G}_i^N(\lambda) = \pi \sum_{\mu=1}^N (\psi_{\mu}^i)^4 \delta(\lambda - \lambda_{\mu}). \quad (\text{A6})$$

By summing the above equation over all the sites and dividing by $N\rho(\lambda)$ we obtain, in the limit $N \rightarrow \infty$, the identity that relates the eigenvalue-dependent IPR with $G_{ii}^N(\lambda - i\epsilon)$ (see eq. (6)). The IPR associated to the state μ is defined as $Y_\mu^N = \sum_{i=1}^N (\psi_\mu^i)^4$. The identity (6) holds only in the absence of degenerate states. In the presence of degenerate states, the function $\mathcal{G}_i^N(\lambda)$ is given by eq. (A6) plus a correction term that involves a sum over all the degenerate eigenvectors.

Appendix B: The cavity method

We show in this appendix how to derive the cavity equations for the normalized complex function $\mathcal{P}_{N,z}(\mathbf{x})$ defined by eq. (11). We focus here on the ensemble of fully-connected Lévy matrices in which $J_{ii} = 0$ for $\forall i$. The values of the nondiagonal elements of \mathbf{J} are i.i.d.r.v. drawn from the Lévy distribution, defined in the subsection III B.

1. Cavity equations

The marginal at site k is defined as follows

$$\mathcal{P}_{N,z}(x_k) = \int \left[\prod_{j \in \partial_k} dx_j \right] \mathcal{P}_{N,z}(\mathbf{x}), \quad (\text{B1})$$

in which ∂_k denotes the set of indices in a row k for which $J_{ij} \neq 0$. Here ∂_k is composed of a number of indices of $O(N)$.

Using eq. (B1) as a starting point, one can derive the following equations

$$\begin{aligned} \mathcal{P}_{N,z}(x_k) &\sim \int \left[\prod_{j \in \partial_k} dx_j \right] \mathcal{P}_{N,z}^{(k)}(\mathbf{x}) \\ &\times \exp \left(-\frac{i}{2} z x_k^2 + i x_k \sum_{j \in \partial_k} J_{kj} x_j \right), \quad (\text{B2}) \end{aligned}$$

$$\begin{aligned} \mathcal{P}_{N,z}^{(l)}(x_k) &\sim \int \left[\prod_{j \in \partial_k \setminus l} dx_j \right] \mathcal{P}_{N,z}^{(k,l)}(\mathbf{x}) \\ &\times \exp \left(-\frac{i}{2} z x_k^2 + i x_k \sum_{j \in \partial_k \setminus l} J_{kj} x_j \right), \quad (\text{B3}) \end{aligned}$$

where $\partial_k \setminus l$ denotes the set ∂_k without site l , and the function $\mathcal{P}_{N,z}^{(i_1, \dots, i_M)}(\mathbf{x})$ is defined on the cavity graph $\mathcal{G}^{(i_1, \dots, i_M)}$. The cavity graph $\mathcal{G}^{(i_1, \dots, i_M)}$ is the subgraph of the original graph \mathcal{G} , in which the nodes i_1, \dots, i_M and all their links with the other nodes have been removed.

In order to close the system of eqs. (B2) and (B3), we make two assumptions which have been used in the context of the cavity method for disordered systems

[31]. First, we assume that the functions $\mathcal{P}_{N,z}^{(i)}(\mathbf{x})$ and $\mathcal{P}_{N,z}^{(i,k)}(\mathbf{x})$ factorize over the sites according to $\mathcal{P}_{N,z}^{(i)}(\mathbf{x}) = \prod_{j \in \partial_i} \mathcal{P}_{N,z}^{(i)}(x_j)$ and $\mathcal{P}_{N,z}^{(i,k)}(\mathbf{x}) = \prod_{j \in \partial_i \setminus k} \mathcal{P}_{N,z}^{(i,k)}(x_j)$, respectively. Second, we assume that, in the limit $N \rightarrow \infty$, the marginals on the cavity graphs fulfill $\mathcal{P}_{N,z}^{(i)}(x_j) = \mathcal{P}_{N,z}^{(i,k)}(x_j) \forall j$.

When inserted in eqs. (B2) and (B3), the above assumptions give rise to

$$\begin{aligned} \mathcal{P}_{N,z}(x_k) &\sim \exp \left(-\frac{i}{2} z x_k^2 \right) \\ &\times \prod_{j \in \partial_k} \int dx_j \mathcal{P}_{N,z}^{(k)}(x_j) \exp(i x_k J_{kj} x_j) \quad (\text{B4}) \end{aligned}$$

$$\begin{aligned} \mathcal{P}_{N,z}^{(l)}(x_k) &\sim \exp \left(-\frac{i}{2} z x_k^2 \right) \\ &\times \prod_{j \in \partial_k \setminus l} \int dx_j \mathcal{P}_{N,z}^{(k)}(x_j) \exp(i x_k J_{kj} x_j). \quad (\text{B5}) \end{aligned}$$

The form of eqs. (B4) and (B5) suggest that they can be solved in a self-consistent way through a Gaussian assumption for the functions $\mathcal{P}_{N,z}^{(k)}(x_i)$ and $\mathcal{P}_{N,z}(x_i)$. The variances of the local marginals $\mathcal{P}_{N,z}(x_i)$ are the diagonal elements of the Green function, as one can note from eq. (13). Thus we make the following Gaussian *ansatz* [13] for the cavity functions $\mathcal{P}_{N,z}^{(l)}(x_k)$

$$\mathcal{P}_{N,z}^{(l)}(x_k) = \sqrt{\frac{i}{2\pi G_{kk}^{N,(l)}(z)}} \exp \left(-\frac{i x_k^2}{2 G_{kk}^{N,(l)}(z)} \right), \quad (\text{B6})$$

where $G_{kk}^{N,(l)}(z)$ are the diagonal elements of the Green function in which row l and column l have been removed. The substitution of the *ansatz* (B6) in eqs. (B4) and (B5) leads to the following self-consistent system of equations

$$G_{ii}^{N,(k)}(z) = \frac{1}{z - g_{N,k}^{(i)}(z)}, \quad (\text{B7})$$

$$G_{ii}^N(z) = \frac{1}{z - h_N^{(i)}(z)}, \quad (\text{B8})$$

for $i = 1, \dots, N$ and for all $k \in \partial_i$. The functions $g_{N,k}^{(i)}(z)$ and $h_N^{(i)}(z)$ are defined as

$$g_{N,k}^{(i)}(z) = \sum_{j \in \partial_i \setminus k} J_{ij}^2 G_{jj}^{N,(i)}(z) \quad (\text{B9})$$

$$h_N^{(i)}(z) = \sum_{j \in \partial_i} J_{ij}^2 G_{jj}^{N,(i)}(z). \quad (\text{B10})$$

The fixed-point solution of eqs. (B7) and (B8) allows one to determine the diagonal elements of the Green function for a single instance of \mathbf{J} , which give access to the DOS and the IPR.

2. The ensemble average

In this subsection we explain how one can perform the ensemble average and derive a self-consistent equation for $W_{\lambda,\epsilon}(\omega)$ by employing a method introduced in [33, 34] for a fully-connected Lévy spin-glass. The method consists in the introduction of a small cutoff γ that makes a distinction between small and large matrix elements. The global contribution of the small matrix elements is taken into account by means of the law of large numbers.

We define the sets of indices that distinguish between weak and strong matrix elements in a certain row i according to

$$\begin{aligned}\zeta_i(\gamma) &= \{j \in \mathbb{N} \cap [1, N] | (J_{ij} < \gamma) \wedge (j \neq i)\}, \\ \bar{\zeta}_i(\gamma) &= \{j \in \mathbb{N} \cap [1, N] | (J_{ij} > \gamma) \wedge (j \neq i)\}.\end{aligned}$$

These definitions allow us to rewrite $g_{N,k}^{(i)}(z)$ and $h_N^{(i)}(z)$ as follows

$$h_N^{(i)}(z) = \sum_{j \in \bar{\zeta}_i(\gamma)} J_{ij}^2 G_{jj}^{N,(i)}(z) + \sum_{j \in \zeta_i(\gamma)} J_{ij}^2 G_{jj}^{N,(i)}(z)$$

$k \in \bar{\zeta}_i(\gamma)$:

$$g_{N,k}^{(i)}(z) = \sum_{j \in \bar{\zeta}_i(\gamma) \setminus k} J_{ij}^2 G_{jj}^{N,(i)}(z) + \sum_{j \in \zeta_i(\gamma)} J_{ij}^2 G_{jj}^{N,(i)}(z)$$

$k \in \zeta_i(\gamma)$:

$$g_{N,k}^{(i)}(z) = \sum_{j \in \bar{\zeta}_i(\gamma)} J_{ij}^2 G_{jj}^{N,(i)}(z) + \sum_{j \in \zeta_i(\gamma) \setminus k} J_{ij}^2 G_{jj}^{N,(i)}(z).$$

In the limit $N \rightarrow \infty$, we can remove the k dependence from the sum over the weak matrix elements because it contains an infinite number of terms. Defining the joint distribution $\Omega_z^{(j)}(\omega)$ of the real and imaginary parts of $G_{ii}^{N,(j)}(z)$ for a fixed j

$$\Omega_z^{(j)}(\omega) = \lim_{N \rightarrow \infty} \frac{1}{N} \sum_{i=1}^N \delta \left[\omega - G_{ii}^{N,(j)}(z) \right], \quad (\text{B11})$$

one can apply the law of large numbers to the contribution coming from the weak matrix elements, leading to

$$\lim_{N \rightarrow \infty} \sum_{j \in \zeta_i(\gamma)} J_{ij}^2 G_{jj}^{N,(i)}(z) = \sigma_\gamma^2 \int d\omega \Omega_z^{(i)}(\omega) \omega, \quad (\text{B12})$$

where σ_γ^2 is the variance of the weak matrix elements [33]

$$\sigma_\gamma^2 = N \int_{-\gamma}^{\gamma} dJ P_\alpha(J) J^2 = \frac{2\gamma^{2-\alpha} C_\alpha}{2-\alpha}, \quad (\text{B13})$$

with the distribution $P_\alpha(J)$ defined by eqs. (25) and (26).

A self-consistent equation for $\Omega_z^{(j)}(\omega)$ is derived by substituting eq. (B7) in (B11). One has to distinguish between two cases. If $j \in \zeta_i(\gamma)$, the function $g_{N,j}^{(i)}(z)$ is equal to $h_N^{(i)}(z)$ for any index i , and as a consequence one obtains $\Omega_z^{(j)}(\omega) = W_{\lambda,\epsilon}(\omega)$. If $j \in \bar{\zeta}_i(\gamma)$, one can follow the discussion of [33] in order to show that $\Omega_z^{(j)}(\omega) = W_{\lambda,\epsilon}(\omega)$. The distribution $W_{\lambda,\epsilon}(\omega)$ fulfills the self-consistent equation

$$\begin{aligned}W_{\lambda,\epsilon,\gamma}(\omega) &= \sum_{k=0}^{\infty} \frac{e^{-c_\gamma} c_\gamma^k}{k!} \int \left[\prod_{l=1}^k d\omega_l W_{\lambda,\epsilon,\gamma}(\omega_l) \right] \\ &\times \int \left[\prod_{l=1}^k dJ_l p_{J,\gamma}(J_l) \right] \\ &\times \delta \left(\omega - \frac{1}{z - \sigma_\gamma^2 \langle \omega \rangle - \sum_{l=1}^k H(\omega_l, J_l)} \right), \quad (\text{B14})\end{aligned}$$

in which $\langle f(\omega) \rangle = \int d\omega W_{\lambda,\epsilon,\gamma}(\omega) f(\omega)$ and

$$H(\omega, J) = J^2 \omega, \quad (\text{B15})$$

$$c_\gamma = \frac{2C_\alpha}{\alpha\gamma^\alpha}, \quad (\text{B16})$$

$$p_{J,\gamma}(J) = \begin{cases} \frac{\alpha\gamma^\alpha}{2|J|^{\alpha+1}} & |J| > \gamma \\ 0 & |J| < \gamma \end{cases}. \quad (\text{B17})$$

The quantity C_α is defined by eq. (28).

Acknowledgments

We would like to thank Andrea Pagnani for a helpful discussion. IN thanks Isaac Pérez Castillo and Tim Rogers for many interesting discussions. FLM thanks Yan Fyodorov for a useful correspondence.

[1] E. P. Wigner, Proc. Cambr. Philos. Soc. **47**, 790 (1951).
[2] O. Bohigas, M. J. Giannoni, and C. Schmit, Phys. Rev. Lett. **52**, 1 (1984).
[3] R. Abou-Chacra, P. W. Anderson, and D. J. Thouless, J. Phys. C: Solid St. Phys. **6**, 1734 (1973).
[4] A. J. Bray and G. J. Rodgers, Phys. Rev. B **38**, 11461 (1988).
[5] J.-Y. Fortin, J. Phys. A: Math. Gen. **38**, L57 (2005).

[6] L. Laloux, P. Cizeau, J. P. Bouchaud, and M. Potters, Phys. Rev. Lett. **83**, 1467 (1999).
[7] J.-P. Bouchaud and M. Potters, arXiv:0910.1205v1 (2009).
[8] I. J. Farkas, I. Derényi, A.-L. Barabási, and T. Vicsek, Phys. Rev. E **64**, 026704 (2001).
[9] M. L. Mehta, *Random matrices and the statistical theory of energy levels* (Academic, New York, 1967).

- [10] G. J. Rodgers and A. J. Bray, *Phys. Rev. B* **37**, 3557 (1988).
- [11] M. Bauer and O. Golinelli, *J. Stat. Phys.* **103**, 301 (2001).
- [12] G. Semerjian and L. F. Cugliandolo, *J. Phys. A: Math. Gen.* **35**, 4837 (2002).
- [13] T. Rogers, I. P. Castillo, R. Kühn, and K. Takeda, *Phys. Rev. E* **78**, 031116 (2008).
- [14] R. Kühn, *J. Phys. A: Math. Theor.* **41**, 295002 (2008).
- [15] T. Rogers and I. P. Castillo, *Phys. Rev. E* **79**, 012101 (2009).
- [16] G. Biroli and R. Monasson, *J. Phys. A: Math. Gen.* **32**, L255 (1999).
- [17] A. Cavagna, I. Giardina, and G. Parisi, *Phys. Rev. Lett.* **83**, 108 (1999).
- [18] D. S. Dean, *J. Phys. A: Math. Gen.* **35**, L153 (2002).
- [19] A. Amir, Y. Oreg, and Y. Imry, arXiv:1002.2123 (2010).
- [20] P. Cizeau and J. P. Bouchaud, *Phys. Rev. E* **50**, 1810 (1994).
- [21] M. Araujo, E. Medina, and E. Aponte, *Phys. Rev. E* **60**, 3580 (1999).
- [22] Z. Burda, J. Jurkiewicz, M. A. Nowak, G. Papp, and I. Zahed, *Phys. Rev. E* **75**, 051126 (2007).
- [23] Y. V. Fyodorov and A. D. Mirlin, *Phys. Rev. Lett.* **67**, 2049 (1991).
- [24] S. N. Evangelou and E. N. Economou, *Phys. Rev. Lett.* **68**, 361 (1992).
- [25] S. Ciliberti, T. S. Grigera, V. Martín-Mayor, G. Parisi, and P. Verrocchio, *Phys. Rev. B* **71**, 153104 (2005).
- [26] P. Cizeau and J.-P. Bouchaud, *J. Phys. A: Math. Gen.* **26**, L187 (1993).
- [27] S. Galluccio, J.-P. Bouchaud, and M. Potters, *Physica A* **259**, 449 (1998).
- [28] M. Politi, E. Scalas, D. Fulger, and G. Germano, **74**, 041129 (2006).
- [29] M. Politi, E. Scalas, D. Fulger, and G. Germano, **73**, 13 (2010).
- [30] M. Mézard and G. Parisi, *Eur. Phys. J. B* **20**, 217 (2001).
- [31] M. Mézard, G. Parisi, and M. A. Virasoro, *Spin Glass Theory and Beyond*, vol. 9 of *World Scientific Lecture Notes in Physics* (World Scientific Pub Co Inc., 1987).
- [32] B. V. Gnedenko and A. N. Kolmogorov, *Limit Distributions for Sums of Independent Random Variables* (Cambridge: Addison-Wesley, 1954).
- [33] I. Neri, F. L. Metz, and D. Bollé, *J. Stat. Mech.* p. P01010 (2010).
- [34] K. Janzen, A. Engel, and M. Mézard, *Eur. Phys. Lett.* **89**, 67002 (2010).
- [35] G. Biroli, G. Semerjian, and M. Tarzia, arXiv:1005.0342v1 (2010).